Modeling of metal–oxide semiconductor: Analytical bond-order potential for cupric oxide*

Li Kun(李 坤)[a], Yang Wen(杨 雯)[b]†, Wei Ji-Lin(魏计林)[a],
Du Shi-Wen(杜诗文)[b], and Li Yong-Tang(李永堂)[b]

[a] College of Applied Science, Taiyuan University of Science and Technology, Taiyuan 030024, China
[b] College of Materials Science and Engineering, Taiyuan University of Science and Technology, Taiyuan 030024, China

(Received 6 December 2013; revised manuscript received 3 January 2014; published online 20 February 2014)

Atomistic potentials for cupric element and cupric oxide are derived based on the analytical bond-order scheme that was presented by Brenner [Brenner D W, "Erratum: Empirical potential for hydrocarbons for use in simulating the chemical vapor deposition of diamond films", *Phys. Rev. B* 1992, **46** 1948]. In this paper, for the pure cupric element, the energy and structural parameters for several bulk phases as well as dimmer structure are well reproduced. The reference data are taken from our density functional theory calculations and the available experiments. The model potential also provides a good description of the bulk properties of various solid structures of cupric oxide compound structures, including cohesive energies, lattice parameters, and elastic constants.

Keywords: cupric oxide, analytical bond-order potential, density functional theory

PACS: 71.15.Mb, 61.50.Ah, 62.20.de **DOI:** 10.1088/1674-1056/23/4/047103

1. Introduction

In recent years, metal–oxide materials have steadily aroused increasing interest because of their properties and various potential applications.[1–4] In particular, cupric oxide (CuO) has shown exciting properties as a catalyst and in solid-state sensors, solar cells, and magnetic storage media owing to its low band-gap energy (1.2 eV), high catalytic activity, non-toxic nature, and abundant resource.[5–10] Besides, CuO and Cu are widely used in chemical mechanical polishing (CMP) technology, which is a primary planarization method that is used to manufacture semiconductor chips because of its demonstrated capability to provide better local and global planarizations of wafer surfaces.[11–14] Therefore, a complete understanding of the physical and chemical properties of CuO on an atomic scale is crucial to the development of these related fields.

The natural tools for modeling material processes based on an atomic level are molecular dynamics (MD) and the Monte Carlo (MC) method.[15,16] Furthermore, in both MC and MD simulations, the analytical potentials play a vital role in calculating the Hamiltonian of systems. Such analytical potentials have been widely used in the previous simulations of covalent materials such as silicon, carbon, and others, as well as in numerous metals and alloys,[17,18] although very few simulations have been done for metal oxide. Actually, metal oxides represent an especially difficult case for atomistic modelling, partly because of their complex electronic structure and intricate mixture of ionicity and covalency. In addition, the devised approximative analytical potentials must be valid not only for equilibrium but also for nonequilibrium configurations.

In order to describe the interatomic interactions of a cupric oxide system, we need to model covalent and metallic bonds within one functional form. Most of the existing simulations for metal oxide use shell-model potentials.[19,20] However, since the three-body interactions are not explicitly taken into account in the shell-model potentials, covalent contributions need to be either neglected or subsumed in the fitting parameters. Thus, the shell model potentials represents a better approach to describing metallic interactions. Purely covalent bonding in elemental semiconductors such as carbon, silicon, or germanium can be well described within the bond-order approach pioneered by Abell[21] and Tersoff,[22] and later extended by Brenner.[23–25] Bond-order formalism was shown to be formally equivalent to the embedded-atom method (EAM), which has been very successfully used to model metallic bonding.[23–25] In Ref. [26], a bond-order potential gives a good description of Cu–Cu interactions of bc and fcc structures. Therefore, it is possible to derive a consistent set of bond-order potentials that describe the cupric oxide compound and its components within a single formalism.

In the present study, a short-ranged bond-order potential is derived to model the covalent and metallic bonds of cupric oxide in one functional form. Moreover, our model is suffi-

*Project supported by the Doctoral Program of Higher Education of China (Grant No. 20111415120002), the National Natural Science Foundation of China (Grant Nos. 11204199, 61178067, and 51135007), the Program for the Outstanding Innovative Teams of Higher Learning Institutions of Shanxi Province, China, and the Youth Foundation of Taiyuan University of Science and Technology, China (Grant No. 20113020).

†Corresponding author. E-mail: wyangtyust@hotmail.com

© 2014 Chinese Physical Society and IOP Publishing Ltd

ciently transferable because our criteria include the descriptions of various structures of the elements and compound system.

The rest of the present paper is organized as follows. In Section 2, the model and the numerical approach are described. The total-energy calculations and the fitting potentials for Cu–Cu, O–O, and Cu–O interactions are discussed independently in Section 3. Our conclusions are given in Section 4.

2. Potential model

In our approach we use a short-range bond-order potential that is similar to the Tersoff–Brenner type,[25] in which the energy is modeled as a sum of pair-like interactions, including an attractive term and a repulsive term. Such a model was also successfully used by Albe *et al.*[27] and Erhart *et al.*[28] in typical compound semiconductor systems of GaAs and ZnO, respectively.

The total potential energy is written as a summation over individual bond energies

$$E = \sum_{i>j} f(r_{ij}) \left[V^{\mathrm{R}}(r_{ij}) - \frac{B_{ij} + B_{ji}}{2} V^{\mathrm{A}}(r_{ij}) \right]. \tag{1}$$

The pair-like repulsive energy $V^{\mathrm{R}}(r)$ and attractive energy $V^{\mathrm{A}}(r)$ are given in the Morse-like form

$$V^{\mathrm{R}}(r) = \frac{D_0}{S-1} \exp[-\beta\sqrt{2S}(r-r_0)], \tag{2}$$

$$V^{\mathrm{A}}(r) = \frac{SD_0}{S-1} \exp[-\beta\sqrt{2/S}(r-r_0)], \tag{3}$$

which depend on dimer bond energy D_0, dimer bond distance r_0, and adjustable parameter S. The parameter β is determined by the ground-state oscillation frequency of the dimer as

$$\beta = k \frac{2\pi c}{\sqrt{2D_0/\mu}},$$

where k is the wave number and μ is the reduced mass.

As we only consider the bond integrals to the next neighbors, it is efficient to restrict the interaction to the next neighbor sphere by a cutoff function

$$f(r) = \begin{cases} 1, & r \le R - D, \\ \dfrac{1}{2} - \dfrac{1}{2} \sin\{\pi(r-R)/(2D)\}, & |R-r| \le D, \\ 0, & r \ge R + D, \end{cases} \tag{4}$$

where D and R are the adjustable quantities.

The bond-order parameter B_{ij} also includes angular dependence, which is necessary to accurately model the deformation of covalent bonds. We use a functional form that is a straightforward extension, as used by Brenner.[25] The angular-dependent term $g(\theta)$ is included in the inner sum of the bond-order function, so that B_{ij} reads

$$B_{ij} = (1 + \chi_{ij})^{-1/2},$$
$$\chi_{ij} = \sum_{k(\neq i,j)} f(r_{ik}) g(\theta_{ijk}) \exp[2\mu_{ik}(r_{ij} - r_{ik})]. \tag{5}$$

Here again the cutoff function is included, while the indices monitor the type dependence of the parameters. The square root dependence of the bond order is chosen to conform with the second-order momentum approximation and is not subjected to adjustment in the fitting procedure. The angular function $g(\theta)$ is given by

$$g(\theta_{ijk}) = \gamma \left(1 + \frac{c^2}{d^2} - \frac{c^2}{[d^2 + (h + \cos\theta_{ijk})^2]} \right). \tag{6}$$

For $c = 0$ this term vanishes and the total potential resembles a short-range embedded-atom-method potential of the Finnis–Sinclair type.[25]

The parameter sets for Cu–Cu and Cu–O derived for our analytical bond-order potential (ABOP) are given in Table 1, and will be discussed in detail in the following sections. The parameter set of O–O interactions in Table 1 is cited from Ref. [28].

Table 1. Parameter sets for our analytical bond-order potential (ABOP).

ij	Cu–Cu	O–O[a]	Cu–O
γ	0.0163	0. 82595	0.0049
S	4.4563	1.3864	3.6
β/Å^{-1}	1.2899	2.3090	1.3046
D_0/eV	2.1345	5.166	5.19
r_0/Å	2.2520	1.2075	1.7135
c	4.988	0.035608	0.5968
d	0.44569	0.046496	0.05
h	0.6931	0.45056	0.9263
μ/Å^{-1}	1.2764	0	1.5
R_{cut}/Å	3.80	2.45	2.7
D_{cut}/Å	0.387	0.2	0.1

[a] Ref. [28].

3. Fitting procedure

The parameter sets for Cu–Cu, O–O, and Cu–O are discussed separately in this section. For pure structures, the experimental and several hypothetical structures are calculated. At the same time, our fitting method needs reference data of total energies of different structures, either from experiments or density functional theory (DFT) calculations. Here, we compute the total energy by the pseudopotential code CASTEP[29] with the ultrasoft pseudopotentials (us-PP) and the generalized gradient approximation (GGA). For all calculated structures, the cutoff energies and k-points ($10\times10\times10$) are chosen to achieve a convergence better than 0.01 eV/atom. The

minimum total energy, lattice constant, and bulk modulus are calculated from energy-volume data. The parameters in the pair-like terms are chosen in accordance to the dimer properties, if possible, while the slope of the energy-bond relation is adjusted to the total energy data by varying S.

Table 2. Energy and structural parameters of different Cu phases, which are calculated using the analytic bond-order potential (ABOP) in comparison with results of experiment, density-functional theory, and ABOP of Ref. [26] (ABOP-Hou). V denotes equilibrium volume (Å^3/atom), a_0 the lattice constant (Å), r_0 the bond length (Å), $E_{\rm coh}$ the cohesive energy (eV), $E_{\rm bond}$ the bond energy (eV), and B the bulk modulus (GPa).

	Experiment	US-GGA	ABOP-Hou	ABOP
Cu_2				
r_0/Å		2.252		2.252
D_0/eV		–2.135		–2.1345
sc-Cu				
V/(Å^3/atom)		13.652		13.998
a_0/Å		2.39		2.41
r_0/Å		2.39		2.41
$E_{\rm coh/atom}$/eV		3.1562		3.134
$E_{\rm bond}$/eV		0.526		0.523
B/GPa		108.02		105.67
bc-Cu				
V/(Å^3/atom)		11.697		11.944
a_0/Å		2.86	2.864	2.88
r_0/Å		2.4768		2.494
$E_{\rm coh/atom}$/eV		3.5917	3.515	3.5813
$E_{\rm bond}$/eV		0.449		0.448
B/GPa		114.53	167.2	104.71
fcc-Cu				
V/(Å^3/atom)	11.761[a]	11.859		11.664
a_0/Å	3.61[a]	3.62	3.605	3.60
r_0/Å	2.553[a]	2.560		2.546
$E_{\rm coh/atom}$/eV	3.490[a]	3.643	3.49	3.643
$E_{\rm bond}$/eV	0.43625[a]	0.455		0.455
B/GPa)	127[a]	140.68	150.3	151.80
hcp-Cu				
V/(Å^3/atom)		11.723		11.723
a_0/Å				
r_0/Å		2.55		2.55
$E_{\rm coh/atom}$/eV		3.621		3.624
$E_{\rm bond}$/eV		0.453		0.453
B/GPa		146.75		147.87
dia-Cu				
V/(Å^3/atom)		18.248		18.248
a_0/Å		5.265		5.265
r_0/Å		2.28		2.28
$E_{\rm coh/atom}$/eV		2.569		2.562
$E_{\rm bond}$/eV		0.642		0.641
B/GPa		64.73		56.59

[a]Ref. [30].

3.1. Cu–Cu

In previous studies, the embedded-atom method (EAM) was usually used to fit Cu–Cu interactions.[30,31] This method offers a very handy formalism with few fitting parameters and yields useful models when only a small section of configuration space is of relevance. As is well known, it turns out to be impossible to reproduce all properties equally well with a single parameter set within one analytical potential scheme. In particular, the EAM is very difficult to use to reproduce the fcc–hcp energy difference realistically. Our analytic bond-order potential (ABOP) overcomes the deficiencies of the EAM model, which will be discussed in the following.

The parametrization for the Cu interaction starts with the Cu–Cu dimer. Since no experimental values for the binding energy D_0 and bond distance r_0 are available, D_0 and r_0 are treated as adjustable parameters. Therefore, we adjust D_0 from -2.0 eV to -2.2 eV, and r_0 from 2.15 Å to 2.35 Å: these values are based on our calculated DFT–GGA results. The final ABOP results of D_0 and r_0 are shown in Table 2, in which energies and structures of different Cu phases are presented with results of ABOP, experiment, and DFT, respectively. It can be found that the ABOP results of D_0 and r_0 of the Cu dimer accord well with the DFT–GGA calculations.

Next, the bulk properties are calculated with ABOP, and the results are compared with experimental results, DFT calculations, and ABOP results of Ref. [26]. The results of different structures, including simple cubic (sc), body-centered cubic (bc), face-centered cubic (fcc, natural stable phase of Cu), hexagonal close packed (hcp), and diamond (dia) structures are displayed in Table 2. As shown in Table 2, the ABOP reproduces the energy very well. And the lattice parameters and bulk moduli are also in reasonable agreement with the reference data, which is illustrated in Fig. 1. By comparing our results with the ABOP-Hou results, it can be found that their results are slightly better than ours for bc and fcc Cu structures. However, our parameter sets satisfy higher transferable requirements because we also verify our model in hcp, sc, and diamond structures.

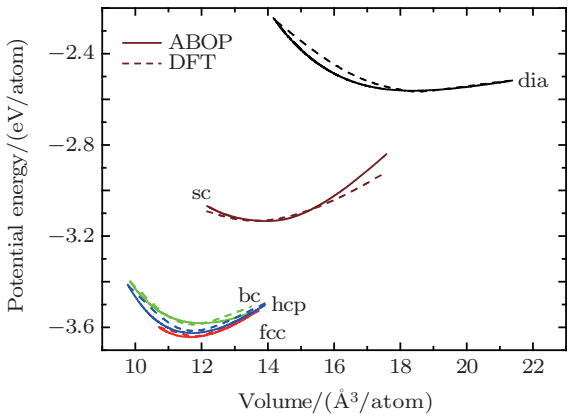


Fig. 1. (color online) Energy–volume curves for bulk structures of Cu, showing a comparison between the results obtained from the ABOP (solid lines) and the reference results obtained by DFT (dotted lines) calculations.

It is worth noting that the ABOP data of potential energy

for the fcc and hcp structures are slightly different, as shown in Table 1 and Fig. 1. Such differences cannot be obtained by other analytical potentials because the energy is mostly determined by the first-neighbor interaction. In our analytical bond-order model, not only the first-neighbor but also the second-neighbor interaction are included in the energy, which leads to the difference in energy between fcc and hcp structures.

3.2. Cu–O

Since the pair parameters of the ABOP are usually adjusted to the dimer data, we begin with properties of the CuO molecule. In a way similar to that of calculating Cu–Cu dimer, we obtain the the binding energy D_0 and bond distance r_0 of Cu–O dimer, the results are listed in Table 3. Table 3 shows that the ABOP data are consistent with the DFT data.

Table 3. Energy and structural parameters of different CuO phases. The experimental values and theoretical results from our DFT calculations are given in comparison with the corresponding numbers as described with the analytical model. The symbols are similar to those in Table 2.

	Experiment	US-LDA+U	ABOP
Cu–O dimer			
r_0/Å		1.7136	1.7135
D_0/eV		–5.206	–5.19
Cu_2O			
V/(Å^3/f.u.)	38.93[a]	39.75	39.48
a_0/Å	4.27[a]	4.30	4.29
r_0/Å	1.85[a]	1.86	1.86
$E_{coh/f.u.}$/eV	–12.88	–13.08	–13.14
E_{bond}/eV	–4.29	–4.36	–4.38
B/GPa	112[a]	93.36	81.704
CuO			
V/(Å^3/f.u.)	20.24[b]	23.54	19.46
a/Å	4.68[b]	4.309	4.88
b/Å	3.42[b]	4.164	3.02
c/Å	5.13[b]	5.256	5.32
α	99.54[b]	93.29	96.84
β	90.0[b]	90.0	90.0
γ	90.0[b]	90.0	90.0
r_0/Å	1.948[b]	1.878	1.974
$E_{coh/f.u.}$/eV	–10.60	–9.32	–10.613
E_{bond}/eV	–2.65	–2.33	–2.65
B/GPa	84.7	99.7	114.91

[a] Ref. [32].

[b] Ref. [33].

For bulk properties, two kinds of solid structures, CuO and Cu_2O are investigated systematically. Due to their technological importance, CuO and Cu_2O are very well characterized, both theoretically and experimentally. The unit cell of CuO is monoclinic and space group is $C2/c$, while the unit cell of Cu_2O is cubic and space group is $Pn3m$. Since CuO is a strongly correlated system, the strong electron–electron interactions in it should be considered in calculation. Therefore, we use LDA + U method in the DFT calculations, and list the results in Table 3.

Table 3 provides an overview of the performance of the ABOP with respect to bulk properties of CuO and Cu_2O, showing the comparison between experimental results and DFT calculations. The parameter set given in Table 1 yields very good agreement with the experimental data as shown in Table 3. Actually, our ABOP results, such as lattice parameters and cohesive energy in Table 3, are even closer to the experimental data than the DFT results. Only the bulk moduli tend to be slightly overrated for the solid structures. However, the overall agreement is at least good. On the other hand, the curve of potential energy versus volume in Fig. 2 also presents the agreement with the DFT results. It should be noted that the deviation of CuO system in Fig. 2 mainly comes from the inaccuracy of the DFT results because CuO is a strongly correlated electronic system.

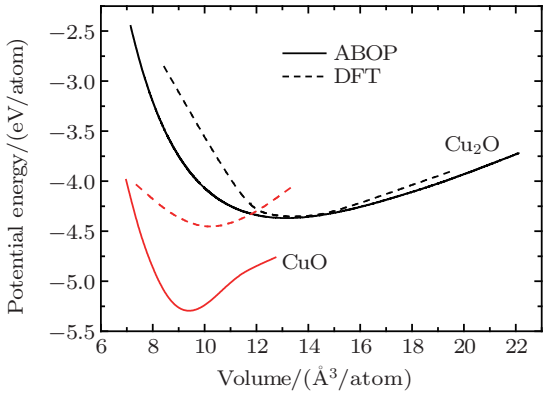


Fig. 2. (color online) Energy–volume curves for bulk structures of Cu–O, showing a comparison between the results obtained from the ABOP (solid lines) and the reference results obtained by DFT (dotted lines).

4. Conclusion

An analytical bond-order potential is derived for modeling a CuO system, which describes different dimer properties and several solid structures of the pure elements and the compound including metastable configurations. Therefore, the present potential is applicable in simulations that require a thermodynamic model for the entire Cu–O system.

Such a potential can model covalent and metallic bonds within one functional form. And since the interatomic potential developed in this work is short-ranged, it is computationally more efficient than the ionic potentials that require the evaluation of long-ranged Coulombic interactions. Thus, it could be extended to other metal oxide or semiconductor compounds.

Acknowledgment

Part of the calculations were carried out in the Center for Computational Science of CASHIPS (China).

References

[1] Park J C, Kim J, Kwon H and Song H 2009 *Adv. Mater.* **21** 803
[2] Li P, Nan C, Wei Z, Lu J, Peng Q and Li Y 2010 *Chem. Mater.* **22** 4232
[3] Zhang H J, Liu Z W, Chen Z Q and Wang S J 2011 *Chin. Phys. Lett.* **28** 017802
[4] Ren J K, Ren Y F, Tian Y, Yu H F, Zheng D N, Zhao S P and Lin C T 2011 *Chin. Phys. B* **20** 117401
[5] Niu F, Jiang Y and Song W 2010 *Nano Res.* **3** 757
[6] Hung L I, Tsung C K, Huang W and Yang P 2010 *Adv. Mater.* **22** 1910
[7] Chen C, Qu J, Cao C, Niu F and Song W 2011 *J. Mater. Chem.* **21** 5774
[8] Gao J, Li Q, Zhao H, Li L, Liu C, Gong Q and Qi L 2008 *Chem. Mater.* **20** 6263
[9] Xu L, Sithambaram S, Zhang Y, Chen C H, Jin L, Joesten R and Suib S L 2009 *Chem. Mater.* **21** 1253
[10] Jiang Z A, Chen J T, Wang J, Zhuo R F, Yan D, Zhang F and Yan P X 2009 *Chin. Phys. Lett.* **26** 086202
[11] Pietsch G J, Higashi G S and Chabal Y J 1994 *Appl. Phys. Lett.* **64** 3115
[12] Zantye P B, Kumar A and Sikder A K 2004 *Mater. Sci. & Eng. R* **45** 89
[13] Ye Y Y, Biswas R, Bastawros A and Chandra A 2002 *Appl. Phys. Lett.* **81** 1875
[14] Ye Y Y, Biswas R, Morris J R, Bastawros A and Chandra A 2003 *Nanotechnology* **14** 390
[15] Jacoboni C and Reggiani L 1983 *Rev. Mod. Phys.* **55** 645
[16] Payne M C, Teter M P, Allan D C, Arias T A and Joannopoulos J D 1992 *Rev. Mod. Phys.* **64** 1045
[17] Pedersen M O, Bonicke I A, Lægsgaard E, Stensgaard I, Ruban A, Norskov J K and Besenbacher F 1997 *Surf. Sci.* **387** 86
[18] Nordlund K, Ghaly M, Averback R S, Caturla M, Diaz de laRubia T and Tarus J 1998 *Phys. Rev. B* **57** 7556
[19] Lewis G V and Catlow C R A 1985 *J. Phys. C: Solid State Phys.* **18** 1149
[20] Binks D J and Grimes R W 1993 *J. Am. Ceram. Soc.* **76** 2370.
[21] Abell G C 1985 *Phys. Rev. B* **31** 6184
[22] Tersoff J 1988 *Phys. Rev. B* **37** 6991
[23] Brenner D W 1989 *Phys. Rev. Lett.* **63** 1022
[24] Brenner D W 1990 *Phys. Rev. B* **42** 9458
[25] Brenner D W 1992 *Phys. Rev. B* **46** 1948
[26] Hou H Y, Wang R S, Wang J T, Liu X B, Chen G and Huang P 2012 *Modelling Simul. Mater. Sci. Eng.* **20** 045016
[27] Albe K, Nordlund K, Nord J and Kuronen A 2002 *Phys. Rev. B* **66** 035205
[28] Erhart P, Juslin N, Goy O, Nordlund K, Muller R and Albe K 2006 *J. Phys.: Condens. Matter* **18** 6585
[29] Segall M D, Lindan P J D, Probert M J, Pickard C J, Hasnip P J, Clark S J and Payne M C 2002 *J. Phys.: Condens. Matter* **14** 2717
[30] Mishin Y, Mehl M J, Papaconstantopoulos D A, Voter A F and Kress J D 2001 *Phys. Rev. B* **63** 224106
[31] Foiles S M, Baskes M I and Daw M S 1988 *Phys. Rev. B* **37** 10378
[32] Ruiz E, Alvarez S, Alemany P and Evarestov R A 1997 *Phys. Rev. B* **56** 7189
[33] Wu D, Zhang Q and Tao M 2006 *Phys. Rev. B* **73** 235206